Electrolytic Preparation of Vanadium(II) Formate in Pilot-Plant Scale Using Stainless Steel Mesh Electrodes: Dissolution of α-Fe $_2$ O $_3$ /Fe $_{1.6}$ Cr $_{0.4}$ O $_3$ in an Aqueous V II NTA Com…

Article

Electrolytic Preparation of Vanadium(II) Formate in Pilot-Plant Scale Using Stainless Steel Mesh Electrodes: Dissolution of ⬚-FeO/FeCrO in an Aqueous V-NTA Complex

V. S. Tripathi, J. Manjanna, G. Venkateswaran, B. K. Gokhale, and V. Balaji

More About This Article

Additional resources and features associated with this article are available within the HTML version:

- Supporting Information
- Access to high resolution figures
- Links to articles and content related to this article
- Copyright permission to reproduce figures and/or text from this article

View the Full Text HTML

Electrolytic Preparation of Vanadium(II) Formate in Pilot-Plant Scale Using Stainless Steel Mesh Electrodes: Dissolution of α-Fe₂O₃/Fe₁.₆Cr₀.₄O₃ in an Aqueous V^II-NTA Complex

V. S. Tripathi, J. Manjanna, G. Venkateswaran,* B. K. Gokhale, and V. Balaji

Applied Chemistry Division, Bhabha Atomic Research Centre, Mumbai 400085, India

The chemical formulations containing strong reducing agents such as V(II) are kinetically effective for the reductive dissolution of iron oxides such as Fe_3O_4, Fe_2O_3, etc. To develop a methodology for large-scale synthesis of V(II), we report here the details of an electrolytic preparation on a pilot-plant scale (50 L). It is demonstrated that, by using stainless steel mesh cathode and anode in a poly(tetrafluoroethylene)-lined stainless steel tank, V(II) could be prepared. To minimize the electrolysis duration for the conversion of V(V) to V(II), laboratory studies are carried out for a preliminary reduction of V(V) to V(IV) with hydrazine or ascorbic acid and then employing V(IV) for electrolysis. Here, the use of hydrazine was advantageous (30% less time) over that of ascorbic acid. The V(II) obtained was complexed with nitrilotriacetic acid (NTA), and its stability and dissolution kinetics of Fe_2O_3 and $Fe_{1.6}Cr_{04}O_3$ in the V^II-NTA formulation are reported.

Introduction

Strong reducing reagents such as vanadium(II) complexes are used for the reductive dissolution of iron(III) oxides,[1,2] normally encountered as corrosion products on the structural surfaces such as stainless steel, carbon steel, etc., especially under high-temperature hydrothermal conditions. In water-cooled nuclear power reactors, the chemical decontamination of system materials using vanadous reagents/formulations is very attractive in terms of achieving rapid radioactivity removal. The radiation-field buildup on the system materials is due to the activity transport phenomenon, wherein the corrosion products when transported through the core undergo neutron activation and deposit on the out-of-core regions of the pipelines of the recirculation system.[1] The nature of corrosion products depends on the type of structural material as well as the coolant chemistry environment practiced in the operating power plants. Nevertheless, iron oxides form the major part when compared with other oxides such as Cr_2O_3, NiO, etc. While the simple iron oxides such as Fe_3O_4, $γ\text{-}Fe_2O_3$, $FeOOH$, $α\text{-}Fe_2O_3$, etc., can be efficiently dissolved using organic acid based formulations such as a mixture of citric acid, ethylenediaminetetraacetic acid (EDTA), and ascorbic acid (CEA),[3] the Cr- and Ni-substituted iron oxides such as $Fe_{2-x}Cr_xO_3$, $Fe_xCr_yNi_zO_4$ ($x + y + z = 3$), etc., require formulations involving stronger reducing agents such as V^II-EDTA, V^II(pic)₃, etc.[1-4] Although V(II)-based reagents have been used for the chemical decontamination of subsystems in some of the reactors,[4] to our knowledge, the details of V(II) preparation at large scale have not yet been reported. However, the electrolytic reduction of V(V) to V(II) on laboratory scale (qualitative) using different cathode materials such as Hg[5-7] and a carbon-based composite[8,9] has been reported. However, the use of significant quantities of Hg as the cathode for large-scale V(II) preparation poses

problems of toxicity, handling, etc. Similarly, the use of a carbon-based cathode requires special preparation and handling precautions. Hence, it is felt that these materials are not easy to use when large-scale preparation for a real system application is to be carried out. For instance, the chemical decontamination of the recirculation system of a 220 MWe boiling water reactor requires thousands of liters of formulation. Thus, in our efforts toward an alternative electrode material for such an application, we have found that stainless steel mesh could serve this purpose. Our earlier explorative studies done with this material and some other materials have been reported elsewhere.[10] In this paper we report the pilot-plant-scale preparation of vanadium(II) formate using an in-house-designed poly(tetrafluoroethylene) (PTFE)-lined stainless steel tank as an electrolytic cell. Also, some laboratory-scale studies have been done on the chemical reduction of V(V) to V(IV) using ascorbic acid and hydrazine. The V(IV) thus obtained was subjected to electrolysis, and by following this strategy, we could save about 30% of the electrolysis time. Furthermore, we report the complexation of V(II) with nitrilotriacetic acid (NTA) and the dissolution behavior of the corrosion products such as hematite/Cr-substituted hematite in the V^II-NTA/NTA formulation.

Experimental Section

Design of Electrolytic Cell/Electrodes. Circular stainless steel (AISI 304 grade) mesh sheets (four layers, well separated) encased in a stainless steel frame were used as a cathode. In the case of the anode, the stainless steel meshes were rolled (four layers) in the form of concentric cylinders with circular stainless steel rings at both ends to provide stability. A 60 L capacity stainless steel tank (internally lined with PTFE, ~0.5 mm thickness to prevent metal-surface-catalyzed conversion of V^{2+} to V^{3+}) wherein the cathode rested at the bottom of the cell while the anode was kept in a separate compartment (using a high-density polyethylene pipe) mounted from the top lid (Figure 1) constituted the electrolytic cell. A G-3 sintered-quartz disk was placed at the bottom portion of the anode compartment to

* To whom correspondence should be addressed. Tel.: +91-22-2559 3866. Fax: +91-22-2550 5151. E-mail: gvenk@magnum.barc.ernet.in.
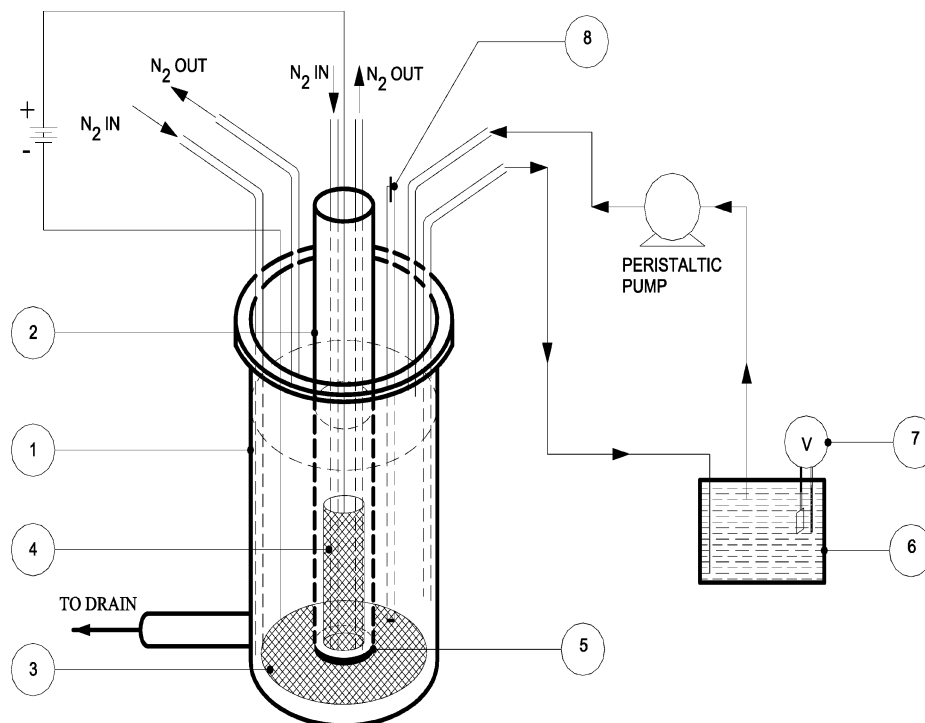
Figure 1. Electrolytic cell setup for V(II) preparation in pilot-plant scale: (1) cathode compartment; (2) anode compartment; (3) cathode; (4) anode; (5) G-3 sintered disk separating anodic and cathodic compartments; (6) solution potential measurement cell; (7) solution potential measurement using a platinum electrode and SCE; (8) arrangement for measuring the cathode potential.

separate the anolyte and catholyte. The distance between the anode and cathode was kept at a minimum (~10 cm) to achieve maximum current efficiency. The anode and cathode were connected to dc power supply unit (0−200 V) using stainless steel wires. The N_2 gas was purged through both the anolyte and catholyte throughout the electrolysis. In the cathode compartment, N_2 was purged in such a way that it provided a sweeping effect to reduce the cathodic polarization due to the H_2 generated on the cathode. The H_2 thus removed from the cathode was let out of the electrolytic cell along with N_2 through an outlet provided for the same. Furthermore, a provision was made to circulate the catholyte as shown in Figure 1 to facilitate the solution potential measurement to monitor the electrolysis. The cathode potential was measured between the cathode terminal of the power supply unit and the standard calomel electrode (SCE) mounted close to the surface of the cathode mesh in the cathode compartment.

Electrolysis. Prior to a pilot-plant-scale demonstration of V(II) preparation, a few cyclic voltammetry experiments on stainless steel electrode (having a circular surface area of around 0.2 cm²) were carried out to establish an approximate reduction potential for VO^{2+} (arising from the use of sodium metavanadate, $NaVO_3$, in a formic acid medium) on a stainless steel electrode. The cyclic voltammograms obtained with a stainless steel electrode have been compared with the one obtained by using Hg as the working electrode (spherical surface area of the Hg drop electrode: ~2.4 × 10⁻³ cm²). Subsequently, in the pilot-plant scale, $NaVO_3$ (~20 mM) in a formic acid (~170 mM) medium was used as the catholyte, pH ~ 2.8, and an equimolar mixture/buffer of HCOOH and NaOH was taken as the anolyte (~170 mM). The deoxygenation was performed in all experiments by continuous purging of high-purity N_2 gas. The concentration of HCOOH and/or pH of both

the anolyte and catholyte was periodically measured and maintained to avoid any precipitation and also to keep the medium sufficiently conducting. The total concentration of formic acid was estimated after passing a sample solution through the cation exchanger and titrating against NaOH. The total formic acid concentration thus estimated was corrected for the V species concentration considered on an equivalent basis so as to arrive at the concentration of free formic acid. Also, from the measured pH value of the catholyte, the concentration of free formic acid was calculated, which showed an agreement with the measured values by titrimetry. The electrolysis was monitored by measuring the solution potential. As the reduction progressed, it was accompanied by a color change from yellow [V(V)] to sky blue [V(IV)] to green [V(III)] and at the end purple [V(II)]. At the end of electrolysis, the UV−visible spectra and solution potential of the vanadium(II) formate as well as its complex with the chelating agent NTA were recorded over a period of 1 month to assess its stability under airtight conditions.

Dissolution Studies. Hematite (Fe_2O_3) and Cr-substituted hematite ($Fe_{1.6}Cr_{0.4}O_3$) were chosen for dissolution because the former is a typical corrosion product on carbon steel surfaces under oxidative chemical environment like the one existing in boiling water reactors operating under normal water chemistry conditions while the latter is a solid solution that can arise from austenitic stainless steel. These oxides were prepared by heating the corresponding hydroxide or coprecipitated hydroxides in air at 1073 K for 4 h and well characterized as described in our earlier studies.[11] Different amounts of oxides were subjected for dissolution in a 20 mM V^{II}-NTA formulation at 353 K in deoxygenated conditions containing enough NTA for complexation of dissolved metal ions. The periodically collected samples were filtered through a 0.45 μm filter paper, and the dissolution course was followed by
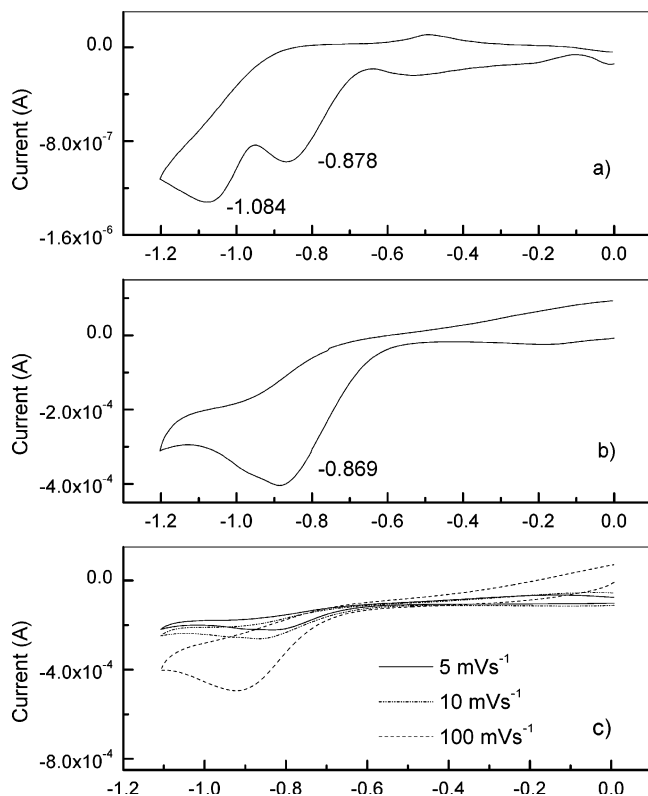
Figure 2. Cyclic voltammogram of 1 mM NaVO$_3$ and 8 mM HCOOH obtained in 0.5 M KNO$_3$ with (a) a Hg electrode, (b) with a stainless steel electrode (scan rate: 100 mV s^{-1}), and (c) with a stainless steel electrode with varying scan rates.

estimation of iron spectrophotometrically using o-phenanthroline as a complexing agent.

Results and Discussion

Electrolytic Preparation of V(II) on a Stainless Steel Mesh Electrode. The reduction peak potential of the formation of vanadium(II) formate on a stainless steel electrode was found to be around −0.87 V vs SCE as determined by cyclic voltammetric run (Figure 2). This peak potential was assigned for the direct reduction of V(IV) to V(II). Barrado et al.[12] have studied the electrochemical behavior of V compounds at a carbon paste electrode in detail. They have observed the reduction process for the conversion of V^{5+}→ V^{4+} (R$_1$) and V^{4+}→ V^{2+} (R$_3$) and the oxidation process for V^{2+}→ V^{3+}-(O$_1$), V^{3+}→ V^{4+} (O$_2$), and V^{4+} → V^{5+} (O$_3$) at a scan rate of 0.5 mV/s, at potentials (V vs Ag/AgCl), viz., 0.71 (R$_1$), −0.54 (R$_3$), −0.35 (O$_1$), 0.46 (O$_2$), and 0.91 (O$_3$), respectively, for NaVO$_3$ dissolved in a 1 M perchloric acid medium. The complexity of V electrochemistry, for example, a shift in peak potentials with different cathode materials and the acidity of the media (pH variation), has been reported in many studies.[12−16] In the present study (Figure 2), the reduction peak for V(IV) to V(II) alone could be observed, and it seems to behave irreversibly because there are no oxidation peaks observed in the reverse scan. The irreversible nature of V(IV) to V(II) reduction in this system was further characterized by varying scan rates, wherein the negative shift in the cathodic peak potential was observed with increasing scan rate (Figure 2c). The scan rate was varied from 5 to 100 mV s^{-1}. As can be seen in Figure 2b, a broad peak was observed on stainless steel when compared to the two separate peaks observed on the Hg electrode. This is essentially due to the unavoidable H$^+$
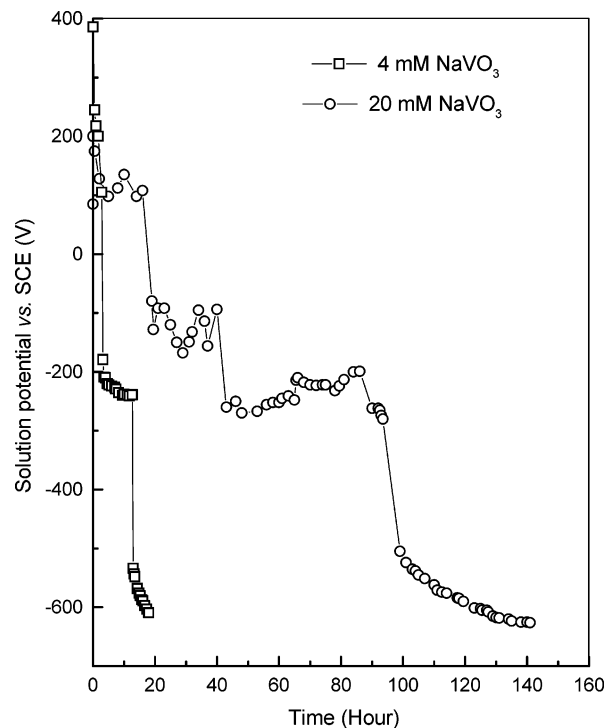

Figure 3. Variation in the solution potential with time during electrolysis of NaVO$_3$ at pilot-plant scale (50 L) under deaerated conditions.
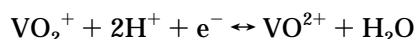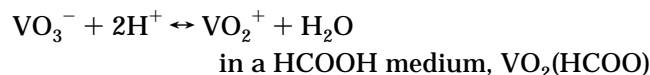
reduction on the stainless steel electrode, which starts occurring at much lower potentials as compared to that on Hg. Upon consideration of material(s) compatibility toward the implementation of V(II) preparation on a large scale, we have restricted our studies only to a formic acid medium.

In the pilot-plant-scale preparation, electrolysis was done with a cathode potential in the range of −1.0 to −1.5 V vs SCE. This applied potential was kept higher than the potential established by cyclic voltammetry to take care of the voltage drop between the reference electrode and the cathode. In fact, when the cathode potential of −0.9 V was maintained, the cell current was negligible. However, with an increase in the potential to a more negative value than −1.0 V, there was a significant increase in the cell current (∼ 1.0 A). At potentials more anodic to −1.5 V, the H$_2$ evolution (due to H$^+$ reduction in the cathode compartment) increased, resulting in an increase of the pH of the catholyte. Thus, we arrived at the value of −1.0 to −1.5 V to be held as cathodic based on our earlier trials. The pH and HCOOH concentration in the catholyte were periodically monitored and maintained to avoid precipitation of V species. The electrolysis was monitored by measuring the solution potential of the circulating solution. Figure 3 shows a decrease in the solution potential with electrolysis time. A potential of −0.625 V shows the near completion of electrolysis (>95% conversion to V^{2+}). The concentration of V(II) was estimated upon titration with standard permanganate solution at ambient temperature conditions:

$$5V^{2+} + 3MnO_4^- + 24H^+ \ (10\% \ H_2SO_4) \rightarrow$$
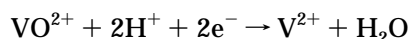$$5V^{5+} + 3Mn^{2+} + 12H_2O$$
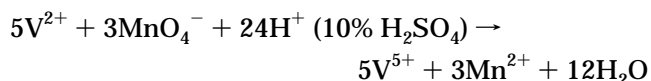
In the presence of both V(II) and HCOOH, at ambient temperatures (301 K), it is the V(II) owing to its strong

reducing nature that reacts preferably with permanganate. The reaction of formic acid with permanganate is slow at room temperature. Nevertheless, in the estimation of the V concentration, a blank correction is applied by titrating a simple formic acid solution of concentration equal to that found in the catholyte at the end of electrolysis. Analysis of the catholyte at the end of electrolysis showed that the stainless steel mesh had not released any iron or other structural metal like Cr and Ni into the medium by corrosion. During electrolysis, the stepwise reduction of VO_2^+ to V^{2+} can be represented by the following equations.

$$NaVO_3 \rightarrow Na^+ + VO_3^-$$
$$\text{on dissolution in an aqueous medium}$$

$$VO_3^- + 2H^+ \leftrightarrow VO_2^+ + H_2O$$
$$\text{in a HCOOH medium, } VO_2(HCOO)$$

$$VO_2^+ + 2H^+ + e^- \leftrightarrow VO^{2+} + H_2O$$

VO^{2+} is directly and irreversibly reduced to V^{2+} as

$$VO^{2+} + 2H^+ + 2e^- \rightarrow V^{2+} + H_2O$$

Also, V^{2+} thus generated reduces VO^{2+} to V^{2+} and in the process gets oxidized to V^{3+} as

$$2V^{2+} + VO^{2+} + 2H^+ \rightarrow 2V^{3+} + V^{2+} + H_2O$$
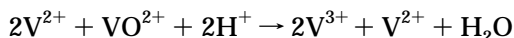
Then V^{3+} is reduced to V^{2+} as $V^{3+} + e^- \leftrightarrow V^{2+}$.

Because of H^+ reduction on the stainless steel mesh, the reduction of V had a lower current efficiency ($\sim$60–70%). On the basis of the amount of the charge passed, it is estimated that $\sim$30–40% of the cell current was consumed by the unavoidable H^+ reduction. When there was an all-around N_2 sweeping arrangement through the mesh cathode, the polarization effects due to H_2 evolution on the cathode could be minimized.

To shorten the time taken for electrolysis in pilot-plant scale, we have adopted a different strategy for the preparation in which V(V) was preliminarily reduced chemically to V(IV) in a formic acid medium and then employed for electrolysis. For this purpose, reducing agents such as ascorbic acid and hydrazine were tried in the laboratory scale (with $\sim$500 mL of electrolyte). Although the V(IV) salts such as $VOSO_4$ are commercially available, they could not be used because sulfate or chloride ions are detrimental to the real system application (i.e., water-cooled nuclear reactors). Hence, as an alternative method, reducing agents (ascorbic acid and hydrazine) were tried because these chemicals are compatible with the structural material of nuclear reactors. The selection of ascorbic acid and hydrazine is also due to their ability to scavenge dissolved oxygen apart from their reductive action. In an acidic medium, the following reduction couples are considered:

$$O_2 + 4H^+ + 4e^- \rightarrow 2H_2O \qquad E° = 1.228 \text{ V vs SHE}$$

$$N_2 + 5H^+ + 4e^- \rightarrow N_2H_5^+ \qquad E° = -0.23 \text{ V vs SHE}$$

$$A \text{ (dehydroascorbic acid)} + 2H^+ + 2e^- \rightarrow$$
$$H_2A \text{ (ascorbic acid)} \qquad E° = 0.400 \text{ V vs SHE}$$
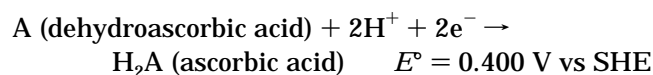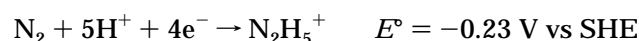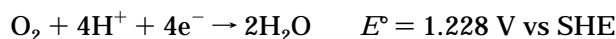
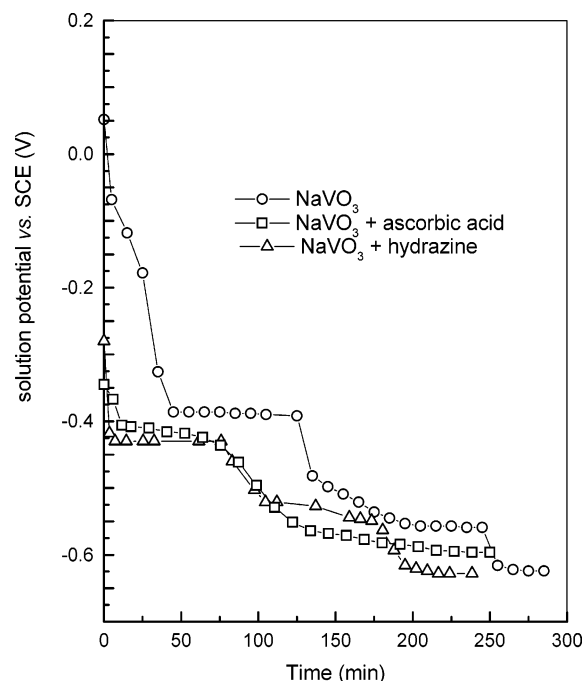Also, they are used as constituents of the decontamina-

Figure 4. Variation in the solution potential with time during electrolysis of 20 mM NaVO$_3$ at laboratory scale (570 mL) under various chemical conditions.

tion formulation for the reductive dissolution of iron-(III) oxides. The stoichiometric amount of ascorbic acid or hydrazine was used considering ascorbic acid as a two-electron reductant and hydrazine as a four-electron reductant. In the case of ascorbic acid, the reduction of V(V) to V(IV) was instantaneous (rapid kinetics) even at room temperature (298 K), while with hydrazine, the reduction was found to be effective at temperatures of >343 K. In a typical case of a 20 mM NaVO$_3$ solution in a formic acid medium, the reduction of V(V) to V(IV) by hydrazine took about 20 min. The reduction was confirmed by a shift in the solution potential to a stable value, e.g., from +248 to −380 mV vs SCE in the case of ascorbic acid and from +248 to −200 mV vs SCE in the case of hydrazine, apart from the visual color change, i.e., yellow to sky blue.

The vanadium(IV) formate thus obtained through a chemical method was employed for the electrolysis in the laboratory scale on a stainless steel mesh electrode and compared with the electrolysis of aqueous NaVO$_3$. It is clear from Figure 4 that there was a significant decrease in the electrolysis time on the hydrazine addition, i.e., $\sim$30% less time when compared to the case of electrolysis done without any preliminary reduction. With ascorbic acid addition, there was a strong interference from the oxidation product of ascorbic acid in the reduction process and the solution potentials could not reach the values obtained in the case of hydrazine addition. Thus, there is no advantage with the use of ascorbic acid. Contrary to ascorbic acid, the oxidation products of hydrazine are gaseous and hence they do not interfere. Thus, the preliminary chemical reduction step using hydrazine enables the preparation of V(II) from V(IV) instead of V(V). The 30% reduction in the electrolysis duration thus obtained can nearly counteract the reduction in the current efficiency (about 30–40%) observed for V(II) generation from V(V) because of simultaneous hydrogen evolution occurring on stainless steel electrodes. Thus, we believe that by introduction of a preliminary reduction step V(II) can be
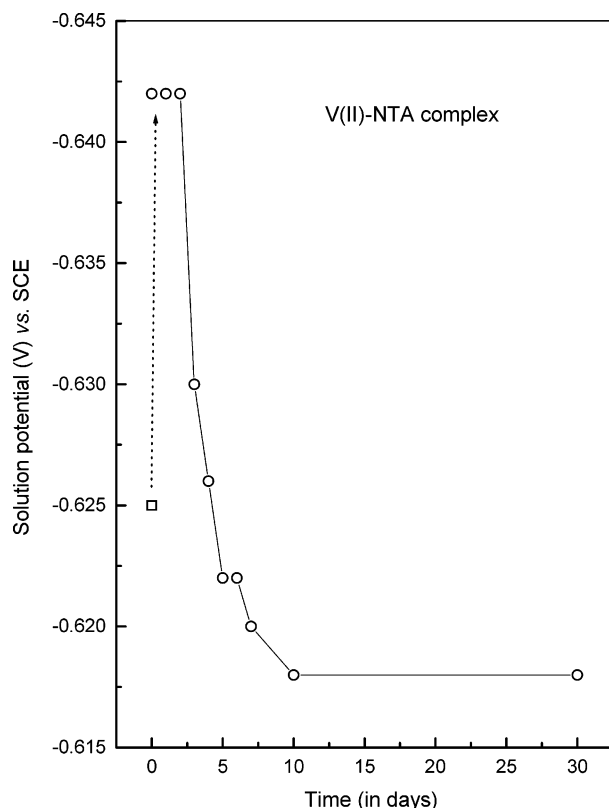
Figure 5. Shift in the solution potential of 20 mM V^{II}-NTA over a period of time after electrolysis under deaerated conditions.
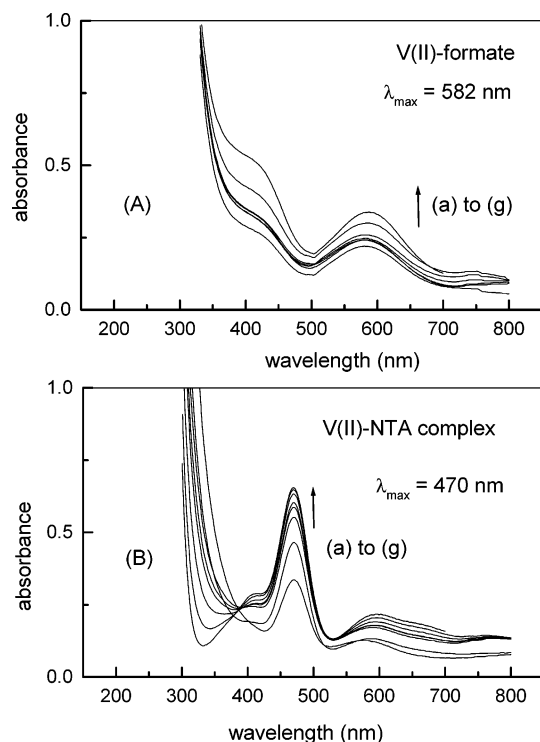

Figure 6. UV–visible spectra of an aqueous vanadium(II) formate/NTA solution at different intervals of time, viz., (a) a fresh solution and of a stored solution (airtight) for (b) 1, (c) 2, (d) 3, (e) 4, (f) 10, and (g) 30 days.

electrolytically prepared using stainless steel mesh electrodes in as nearly efficient manner as is possible with the Hg pool cathode, which has a high hydrogen overpotential. The added advantages of the low cost of stainless steel and its environmentally benign nature compared to Hg seem to make it a more viable cathodic material for large-scale applications. Thus, V(II) can be prepared efficiently on a cost-effective, environmentally benign, and user-friendly stainless steel electrode by the above electrochemical route.

Complexation of V(II) with NTA. An aliquot of vanadium(II) formate obtained after electrolysis in the pilot-plant scale was complexed with NTA. The solution potential (Figure 5) and the UV–visible spectra (Figure 6) of vanadium(II) formate before and after complexation with NTA were recorded. Upon addition of a stoichiometric amount of NTA to vanadium(II) formate, the solution potential shifted from −0.625 to −0.642 V. Similarly, the absorption maxima, λ_{max}, had shown a blue shift, i.e., from 582 to 470 nm upon addition of NTA. This shows the formation of a V^{II}-NTA complex. Because V(II) and its complexes are highly unstable under oxygenated conditions ($4V^{2+} + O_2 + 4H^+ \rightarrow 4V^{3+} + 2H_2O$), the stability of the V^{II}-NTA complex was monitored in airtight and deaerated conditions over a period of several days by periodic recording of the UV–visible spectra and the solution potential, respectively. As can be seen in Figure 6, the absorption spectra show a continuous increase in absorbance with time. This is essentially due to V(II) oxidation by water followed by V(III) complex formation. Both V(II) and V(III) species have three overlapped absorption bands.[17] The increase in the absorbance in the entire spectral region can be attributed to the buildup of V(III) in solution. This also indicates that both vanadium(III) formate and V^{III}-NTA have higher molar extinction coefficients than the

corresponding V(II) species. The increasing solution potential values (Figure 5) also corroborate the decreasing concentration of V(II) observed under airtight conditions (UV–visible spectrophotometry), suggesting the decay of V(II) through water reduction ($V^{2+} + H^+ \rightarrow V^{3+} + ^1/_2H_2$). For up to 3 days, the solution potential of V^{II}-NTA was steady, but in the following 7 days, a new steady state, which is by 24 mV more positive (−0.618 mV vs SCE) with respect to the initial potential −0.642 mV (vs SCE), was reached. A shift of this magnitude accounts for conversion of around 60% of V(II) to V(III), thereby reducing the starting V^{II}-NTA concentration from 20 to 8 mM in about 10 days. The initial stable period of 3 days is quite sufficient with respect to its application after preparation for oxide dissolution. The strong reducing nature of the V(II) formulations is its basic advantage when compared to organic acid based formulations such as CEA.[18]

Dissolution Studies. NTA is more advantageous than other chelating agents such as EDTA. NTA has higher solubility[19] (∼9 mM at 300 K and at a pH of 2.3) in water than EDTA (∼2 mM at a pH of 2.3), and hence higher solution concentrations of NTA could be maintained in nonregenerative multicycle processes of chemical decontamination. Further, the Fe^{III}-NTA complex can be reduced to Fe^{II}-NTA by ascorbic acid.[19,20] The Fe^{II}-NTA thus obtained can further participate in the reduction of $Fe^{3+}\}_{oxide}$ to $Fe^{2+}\}_{(aq)}$, thereby enhancing the dissolution.[20] The catalytic effect of Fe^{II}-NTA is similar to that of Fe^{II}-EDTA reported elsewhere.[21] However, such a reductive action of ascorbic acid was not found with Fe^{III}-EDTA[19,22] because of its high stability (log K = 25.0[23] as compared to 15.9 for Fe^{III}-NTA[23]). In the nonregenerative mode of decontamination, the ion-exchange behavior of the dissolved metal complex plays an important role in the processing of the spent formulation at the end of the decontamination campaign. The
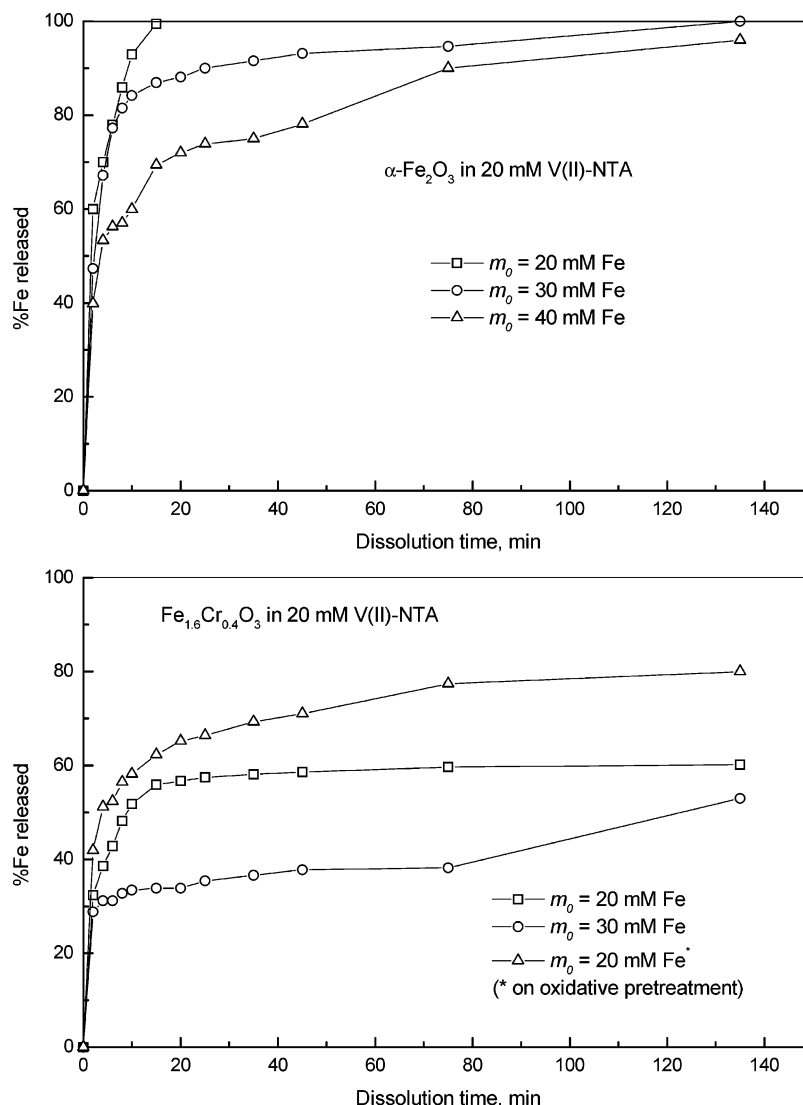
Figure 7. Dissolution profiles of hematite and Cr-substituted hematite (20 atom %) in the V^{II}-NTA formulation at 353 K.

Fe^{III}-NTA complex, unlike the Fe^{III}-EDTA complex and also the Ni^{II}-EDTA complex, breaks significantly on the cation-exchange resin, releasing NTA, which can be taken up on the anion resin.[24] This property of dissociation of the Fe^{III}-NTA complex on the cation resin helps metal ions to get sorbed onto the cation resin, which is more desirable than metal ions getting picked up as anionic complexes on the anionic resin. NTA, unlike EDTA, exhibits a lesser tendency to be removed by a cation exchanger as a protonated species because its protonation constant is 0.1 as compared to that of EDTA with a protonation constant of 38. At a pH of 1.4, ~17 times more EDTA than NTA is picked up by the cation resin as protonated species.[19] This property of NTA is helpful for a regenerative mode of dilute chemical decontamination wherein a cation exchanger in the circuit removes the metals through the dissociation of metal−ligand complexes. The free NTA released on the cation resin gets protonated to a lesser extent and, therefore, unlike EDTA, will be removed to a lesser extent by the cation resin. Hence, a formulation combining V^{II}-NTA, NTA, and ascorbic acid could be a useful decontamination formulation especially for the nonregenerative multicycle mode of decontamination carried out in systems where no base metal participation is

possible such as the stainless steel based primary systems of boiling water and pressurized water reactors.

Manjanna and Venkateswaran[3] have reported the dissolution behavior of Cr-substituted hematite and magnetite in V(II) complexes, viz., vanadium(II) picolinate, V^{II}-EDTA, and vanadium(II) citrate. In this study, the dissolution efficiency of V^{II}-NTA/NTA for corrosion products such as hematite and Cr-substituted hematite is shown in Figure 7. In the case of unsubstituted hematite (α-Fe$_2$O$_3$), a complete dissolution was achieved for different amounts of oxide. When the oxide amount was stoichiometric (20 mM Fe) with the V^{II}-NTA containing an equal amount of free NTA concentration for complexation with iron, the dissolution was complete in about 20 min. In those cases wherein more than a stoichiometric amount of oxide was taken, the corresponding amount of extra NTA was provided. Thus, 20 mM V^{II}-NTA could dissolve 30 and 40 mM iron from hematite because of the reductive action of Fe^{II}-NTA as reported in the earlier studies for EDTA. In the case of Cr-substituted hematite (Fe$_{1.6}$Cr$_{0.4}$O$_3$), reacting with a different mechanism, the dissolution was about 80% with a stoichiometric amount of oxide and it further decreased with higher amounts of oxide. The dissolution rate constants determined by the inverse cubic rate law
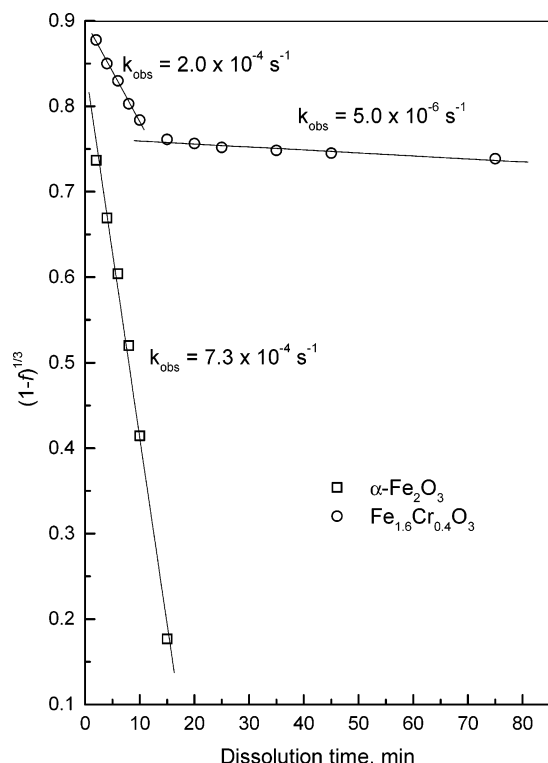
Figure 8. Typical inverse cubic rate law plots for the dissolution of hematite and Cr-substituted hematite.

are shown in Figure 8. Hematite dissolves in a single step, whereas two-stage dissolution was observed with Cr-substituted hematite. This behavior corroborated with the earlier studies reported from our laboratory. Although, according to the dissolution, NTA is comparable with EDTA, the former is preferred in the real system application because of further technological requirements.

Conclusions

The electrolytic preparation of vanadium(II) formate in a pilot-plant scale ($\sim$50 L) was achieved with stainless steel mesh as electrodes. The preliminary chemical reduction of V(V) to V(IV) by hydrazine was found to be effective in shortening the subsequent electrolysis. The formation of a V^{II}-NTA complex and its stability were ascertained by monitoring the solution potential and UV–visible spectra. The use of NTA as a chelating agent is more advantageous than EDTA, although the dissolution efficiency of the V^{II}-NTA/NTA formulation is comparable to that reported for V^{II}-EDTA/EDTA.

Acknowledgment

Literature Cited

(1) Swan, T.; Segal, M. G.; Williams, W. J.; Pick, M. E. *LOMI Decontamination Reagents and Related Preoxidation Process*; Report EPRI NP-5522M prepared by CEGB; Electric Power Research Institute: Berkeley, U.K., 1987.

(2) Segal, M. G.; Swan, T. Chemical Considerations in the Choice of Decontamination Reagents for Water Reactors. *Water Chemistry of Nuclear Reactor Systems 3*; BNES: London, U.K., 1983; p 187.

(3) Manjanna, J.; Venkateswaran, G. Dissolution of Chromium-Substituted Iron Oxides in V(II) Formulations. *Hydrometallurgy* **2001**, *61* (1), 45.

(4) Bradbury, D.; Segal, M. G.; Swan, T.; Comley, G. C. W.; Ferrett, D. J. Decontamination of Winfrith SGHWR coolant circuits using LOMI reagents. *Nucl. Energy* **1981**, *20* (5), 403.

(5) Larkworthy, L. F.; Murphy, J. M.; Patel, K. C.; Phillips, D. J. Vanadium(II) Chemistry. Part I. Magnetic and Spectroscopic Investigation of the Sulphate and Double Sulphates. *J. Chem. Soc. A* **1968**, 2936.

(6) Schaefer, W. P. Acetylacetone Complexes of Vanadium(II). *Inorg. Chem.* **1965**, *4*, 642.

(7) Cotton, F. A.; Falvello, L. R.; Llusar, R.; Libby, E.; Murrillo, C. A. Synthesis and Characterisation of Four Vanadium(II) Compounds, Including Vanadium(II) Sulfate Hexahydrate and Vanadium(II) Saccharinates. *Inorg. Chem.* **1986**, *25*, 3423.

(8) Skyllas-Kazacos, M.; Grossmith, F. Efficient Vanadium Redox Flow Cell. *J. Electrochem. Soc.* **1987**, *134*, 2950.

(9) Haddadi-ASL, V.; Kazacos, M.; Skyllas-Kazacos, M. Conductive Carbon–Polypropylene Composite Electrodes for Vanadium Redox Battery. *J. Appl. Electrochem.* **1995**, *25*, 29.

(10) Gokhale, A. S.; Venkateswaran, G. Electrolytic Preparation of Vanadous Formate/Citrate by using different cathode materials. In *Proceedings of the National Symposium on Water and Steam Chemistry in Power Plants and Industrial Units*; Venkateswaran, G., Gokhale, B. K., Ramshesh, R., Dey, G. R., Eds.; Bhabha Atomic Research Centre: Mumbai, India, 2000; p 111.

(11) Manjanna, J.; Venkateswaran, G. Effect of Oxidative Pretreatment for the Dissolution of Cr-Substituted Hematites/Magnatites. *Ind. Eng. Chem. Res.* **2002**, *41* (13), 3053.

(12) Barrado, E.; Pardo, R.; Castrillejo, Y.; Vega, M. Electrochemical Behavior of Vanadium Compounds at a Carbon Paste Electrode. *J. Electroanal. Chem.* **1997**, *427*, 35.

(13) Israel, Y.; Meites, L. Vanadium. In *Encyclopedia of Electrochemistry of the Elements*; Bard, A. J., Ed.; Marcel Dekker: New York, 1976; Vol. VII.

(14) Dzharkesheva, Z. T.; Zakharov, V. A.; Bekturova, G. B.; Songna, O. A. Voltammetric Study of the Behavior of Vanadium Pentoxide Entering into the Composition of a Mineral-Carbon Paste Electrode. *Izv. Akad. Nauk Kaz. SSR, Ser. Khim.* **1978**, *28*, 30.

(15) Lamache, M.; Bauer, D. Etude, Par Chronoamperometrie, de l'electrode a pate de carbone a liant electrolytique et solide electroactif incorpore. *J. Electroanal. Chem.* **1977**, *79*, 359.

(16) Elouadseri, M. M.; Vittori, O.; Durand, B. Reactivite Electrochmique de Quelques Oxydes de Vanadium en Milieu HCl 1 M. *Electrochim. Acta* **1986**, *31* (10), 1335.

(17) Bennet, R. M.; Holmes, O. G. Electronic States of Hydrated Vanadium(II) Ion. *Can. J. Chem.* **1960**, *38*, 2319.

(18) Manjanna, J.; Venkateswaran, G.; Sherigara, B. S.; Nayak, P. V. Dissolution Studies of Chromium Substituted Iron Oxides in Reductive-Complexing Agent Mixtures. *Hydrometallugry* **2001**, *60* (2), 155.

(19) Rufus, A. L. Study of Ion Exchange Equilibria of Metal Ions on the Substrates Used for the Removal of Radioactive Nuclides from the Coolant Circuits of Nuclear Power Plants. Ph.D. Thesis, University of Madras, Madras, India, 2003.

(20) Venkateswaran, G. Studies regarding the Chemical Decontamination of Recirculation System of TAPS BWRs. Unpublished results.

(21) Manjanna, J.; Venkateswaran, G.; Sherigara, B. S.; Nayak, P. V. Reductive Dissolution of Chromium Substituted Hematites in V(II)-EDTA Formulation. *PowerPlant Chem.* **2001**, *3*, 80.

(22) Ananthan, P.; Venkateswaran, G. Influence of Carbon Steel and Other Structural Materials on the Dissolution of Hematite. *PowerPlant Chem.* **2000**, *2*, 651.

(23) Critical Stability Constants. In *Amino Acids*; Martell, A. E., Smith, R. M., Eds.; Plenum Press: New York, 1974; Vol. 1.

(24) Rufus, A. L.; Velmurugan, S.; Kumar, P. S.; Sathyaseelan, V. S.; Narasimhan, S. V.; Mathur, P. K. Ion Exchange Considerations in Dilute Chemical Decontamination Process Operated in the Regenerative Mode. *Nucl. Technol.* **1998**, *122*, 228.